Turkish Journal of Botany

http://journals.tubitak.gov.tr/botany/

Research Article

Turk J Bot
(2019) 43: 831-849
© TÜBİTAK
doi:10.3906/bot-1903-21

Amanita cinis and *A. olivovaginata* (Basidiomycota, Amanitaceae), two new species, and the first record of *A. emodotrygon*, from Northwestern Pakistan

Sadiq ULLAH[1,3,*], Andrew William WILSON[2,3], Rodham Elliott TULLOSS[4], Muhammad FIAZ[1], Gregory Michael MUELLER[3], Abdul Nasir KHALID[5]
[1]Department of Botany, Hazara University, Dhodial, Pakistan
[2]Denver Botanic Gardens, Denver, CO, USA
[3]Chicago Botanic Garden, Glencoe, IL, USA
[4]Herbarium Amanitarum Rooseveltensis, Roosevelt, NJ, USA
[5]Department of Botany, University of the Punjab, Quaid-e-Azam Campus, Lahore, Pakistan

Received: 17.03.2019 • **Accepted/Published Online:** 26.07.2019 • **Final Version:** 21.11.2019

Abstract: Two new species found in Northwestern Pakistan in the mushroom genus *Amanita* are described and illustrated. Phylogenetic data derived from nuclear ribosomal ITS and LSU regions along with morphological characterizations indicate that these species are novel. *Amanita cinis* is a member of section *Roanokenses,* while *A. olivovaginata* is representative of the section *Vaginatae*. *Amanita emodotrygon*, recently described from the state of Uttarakhand, India, is new to Pakistan.

Key words: Agaricales, Ectomycorrhizae, Himalaya, Mansehra, Shangla

1. Introduction

To date, the genus *Amanita* Pers. comprises about 650 accepted species and is estimated to contain overall 1000 or more species (Yang et al., 2018; Cui et al., 2018). The genus is important because it contains sought-after edible species, but also deadly poisonous species. They are ecologically relevant because the majority of them form ectomycorrhizal associations with vascular plants and play important roles in ecosystems and forest development (Yang, 1997). Taxonomic studies of *Amanita* from Asia have largely focused on China, India, and Japan (Nagasawa and Hongo, 1984; Yang, 1997; Oda et al., 1999; Moncalvo et al., 2000; Tulloss et al., 2001; Chen et al., 2001; Yang, 2001, 2002; Oda et al., 2002; Yang, 2004; Jie et al., 2009; Zhang et al., 2010; Chen, 2014; Deng et al., 2014; Zhang et al., 2015; Yang, 2015; Endo et al., 2017; Cui et al., 2018; Yang et al., 2018). About 60 species of *Amanita* have been reported from various parts of India, and more than 160 species have been reported from China (Yang, 1997, 2000; Semwal et al., 2014; Singh and Kaur, 2016; Cui et al., 2018; Yang et al., 2018). Despite these contributions to the knowledge of *Amanita* in Asia, many regions of the continent remain understudied (Tulloss, 2005).

Pakistan has Himalayan moist temperate forests which are generally suitable for *Amanita* and their ectomycorrhizal partners. The Shangla District of Pakistan lies on the western edge of the Himalayan range and under the Hindukush mountain range with average elevation 2000–3500 m above sea level (asl) (Ullah et al., 2019a). Almost 90% of the area consists of high mountains, with 10% of the area occurring as plains along the Indus river side (Ullah et al., 2019b). Climatically, District Shangla is a moist temperate area (Figure 1), bordering the Himalayan range (Champion et al., 1965). The highest temperature in summer is 38° C, while in winter it goes down to −2 to −5 °C. The observed relative humidity of the area is 65.9% annually (Ullah, 2018). Mansehra District is east of Shangla District, with a similar average elevation (2000–3500 m a.s.l.). The climate is also similar (moist temperate), with seasonal periods of rainfall, snow, and drought. Most of the rainfall occurs during the monsoon season (July–August). The total annual rainfall of the district is 1828 mm, and the temperature ranges from 2 to 36 °C (Fiaz, 2013).

According to the standard classification of forest types of Pakistan, the forests fall under the category "Montane temperate forests" (Champion et al., 1965). The mountains of both districts consist of mostly coniferous forests containing *Pinus roxburghii* Sarg., *P. wallichiana* A. B. Jackson, *Abies pindrow* (Royle ex D. Don) Royle, *Picea smithiana* (Wall.) Boiss., and *Taxus wallichiana* Zucc.

* Correspondence: sadiqbotany@gmail.com

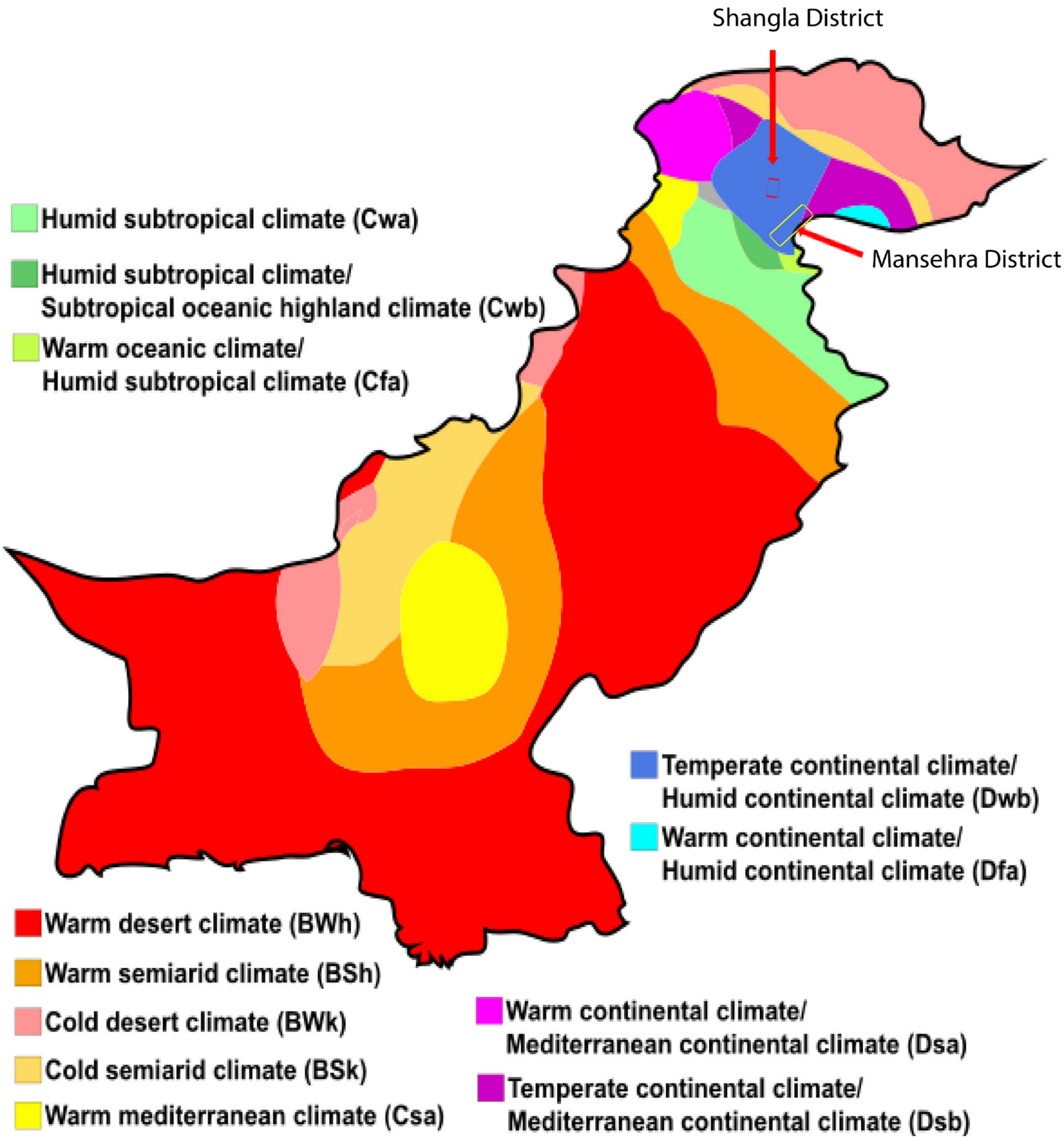

Figure 1. Map of Pakistan based on the Köppen climate classification. The collection sites are given: Shangla District is shown by a rectangle of red boundaries and Mansehra District is shown by a rectangle of yellow boundaries.

Broadleaved tree species include *Aesculus indica* (Wall. ex Camb.) Hook., *Acer caesium* Wall. ex Brandis, *Juglans regia* L., *Quercus incana* Roxb., *Q. semicarpifolia* Smith, and *Ulmus wallichiana* Planch. (Ullah, 2018: Ullah et al., 2019a). The moist temperate climate has in average 1778 mm of precipitation annually (Ullah, 2018). While the habitat is ideal for *Amanita*, few studies of the genus have been done here.

Ahmad (1956) reported a species list containing only 2 taxa of *Amanita* (*A. nana* Sing. and *A. vaginata* [Bull.: Fr.] Lamarck). Tulloss et al. (2001) published 9 taxa of *Amanita* from the Himalayan moist temperate forests of northwestern Pakistan. Niazi et al. (2009) produced a comprehensive report of a rubescent species of section *Validae* (Fr.) Quél. (possibly *A. orsonii* Kumar and Lakhanpal) growing ectomycorrhizal on Himalayan spruce (*Picea smithiana*). Kiran et al. (2017) reported *A. pallidorosea* and its ectomycorrhizal association with *Quercus oblongata*. Jabeen et al. (2017) reported a new species, *A. glarea* S. Jabeen et al., from northwestern Pakistan. More recently, Kiran et al. (2018) reported a new species, *A. griseofusca* J. Khan and M. Kiran, from Swat, Pakistan.

To date, only 15 species of *Amanita* have been documented from Pakistan. This study increases the existing taxonomic knowledge of *Amanita* from Pakistan by describing 2 new species and a new record from the northwestern region of the country using morphological descriptions and molecular phylogenetic data.

2. Materials and methods

2.1. Morphological characterization

Specimens were collected from the Shangla and Mansehra districts (Figure 1) during 2013–2016. Fresh specimens were photographed using a Nikon DS3300 digital camera and tagged. Macromorphological features such as the color of the basidiome, size and shape of the pileus, the stipe, the annulus, volva, lamellar features, and associated vegetation of the area were noted. The specimens were dried and stored in labeled boxes. Color codes were designated using the Munsell Color System (1975). Micromorphological features were described according to Tulloss and Rodríguez-Caycedo (2011). Features were described from sections prepared in 3% KOH, 1% Congo Red, and Melzer's reagent, and observed using a compound light microscope (MX4300H Techno Co., Ltd., Japan) at a magnification of 1000× with oil-immersion. Measurements were recorded using a Carl Zeiss Jena ocular micrometer, and line drawings were made using a camera lucida.

At least 100 basidiospores were measured per species. Values in brackets (= [*a*/*b*/*c*]) represent the number of spores measured (a), per number of basidiomes (b), per number of collections (c). Basidiospores dimensions are shown as (*k*–) *m*–*n* (–*p*) – The values "*m*" and "*n*" represent the 5% and 95% quantiles of spore size distribution (length and width), respectively, with "*k*" as the smallest and "*p*" as the largest observed value. We use the biometric variables defined by Tulloss (Tulloss and Rodríguez-Caycedo, 2011). The value **L** is the range of average spore lengths per specimen examined, and **L´** is the overall average spore length, **W** the range of average spore widths per specimen examined, **W´** is the overall average spore width, Q is the ratio of length/width for one spore, **Q** is the average value of the length/width ratio for spores per specimen examined,; and **Q´** is the average length/width ratio for all spores measured. Biometric variables for describing the lamella trama are also those of Tulloss (Tulloss and Rodríguez-Caycedo, 2011): w_{cs} is the width of the central stratum, $w_{st\text{-}near}$ is the distance from an outer edge of the central stratum to the nearest base of a basidium on the nearest hymenial surface, and $w_{st\text{-}far}$ is the distance from an outer edge of the central stratum to the most distant base of a basidium on the nearest hymenial surface.

The specimens were deposited in the Hazara University Herbarium (HUP), Pakistan, and the LAH Herbarium, Department of Botany University of the Punjab, Quaid-e-Azam Campus, Lahore, Pakistan.

2.2. Molecular analysis

Extractions were obtained from 5–15 mg of dried sporocarp material using a Qiagen DNeasy Plant Mini Kit (Qiagen, Valencia, CA, USA. http://www.qiagen.com/). PCR and cycle sequencing were performed to obtain sequences of nuclear ribosomal internally transcribed spacer regions ITS1, 5.8S, and ITS2 (ITS) using primer pairs ITS1F/ITS4 or ITS2/ITS3 (White et al., 1990; Gardes and Bruns, 1993). Amplification of the nuclear ribosomal large subunit (LSU) genes was done by the primer pair LR0R/LR5 (Vilgalys and Hester, 1990). A 25 µL volume PCR reaction was performed, containing 9 µL ddH_2O, 12.5 µL PCR master mix, 1.25 µL forward primer, 1.25 µL reverse primer, and 1 µL DNA sample. Amplification protocols and PCR conditions used an initial denaturation step of 2 min at 95 °C, followed by 30 cycles of the following steps: a denature step of 1 min at 95 °C, an annealing step of 30 s at 50 °C, and an extension step of 2 min at 72 °C; the reaction was finalized by a final extension for 5 min at 72 °C. Cycle sequence reaction was performed using the above PCR primers, with separate reactions for forward and reverse primers, and the Big Dye Terminator Kit 3.1 (Applied Biosystems, Foster City, CA, USA) with thermocycler protocols using an annealing temperature of 55 °C. PCR products and cycle sequence reactions were purified using a standard ethanol precipitation prep. DNA extraction, PCR, and cycle sequencing reactions were performed at the Chicago Botanic Garden's Center for Plant Biology and Conservation, Glencoe, Illinois. Sequencing was performed using an ABI-3730-XL DNA Analyzer (Applied Biosystems) in the Pritzker Laboratory at the Field Museum of Natural History, Chicago, Illinois. Sequences produced for this study have been deposited in GenBank.

The sequences were processed, edited, and assembled using Codon Code Aligner 3.5 and Bioedit 7.0. They were then screened for percentage sequence identity using a BLAST search of GenBank and UNITE databases. Nearest matches from both databases were downloaded for phylogenetic analysis. Automated alignment of individual ITS and LSU datasets (Table) was done using MUSCLE 3.8 (Edgar, 2004), followed by additional manual alignment in MESQUITE 2.75 (Maddison and Maddison, 2005). The nucleotide alignments were deposited as Nexus files in TreeBASE (23906).

Phylogenetic inference was conducted using Bayesian and maximum likelihood (ML) methods. For Bayesian inference, we used BEAST 1.8.4 (Drummond and Rambaut, 2007) with a Markov chain Monte Carlo (MCMC) coalescent approach. A Yule tree prior (Gernhard, 2008) was used in all simulations, and the starting tree was randomly generated. Four independent runs were undertaken. Chain length was 10 million generations,

Table. Taxa of *Amanita* included in molecular analyses, with voucher specimen ID numbers, country of origin, GenBank accession numbers and references.

Taxon	Voucher	Location	GenBank accessions		References
			LSU	ITS	
A. cinis	SUA752B	Pakistan	MF491876	MF489727	This study
A. cinis	SUA733	Pakistan	MF491878	MF489726	This study
A. cinis	SUA752A	Pakistan	MF491877	MF489725	This study
A. smithiana	RET 382-6	USA	HQ539740	-	Wolfe et al., 2012
A. smithiana	JLF2660	USA	-	MK285662	Data from GenBank
A. polypyramis	RET 159-8	USA	HQ539723	-	Wolfe et al., 2012
A. proxima	RET 290-10	France	HQ539728	-	Wolfe et al., 2012
A. proxima	KT71212AP	Cyprus	-	MH603601	Loizides et al., 2018
A. kotohiraensis	ASIS25144	Korea	KU139463	-	Data from GenBank
A. kotohiraensis	MHHNU 6998	China	FJ011681	FJ176722	Zhang et al., 2010
A. kotohiraensis	HKAS100577	China	-	MH508415	Cui et al., 2018
A. minutisquama	HKAS 100504	China	-	NR_159582	Cui et al., 2018
A. macrocarpa	32531I	China	-	KC408380	Deng et al., 2014
A. neo-ovoidea	HKAS84931	China	MH486655	-	Cui et al., 2018
A. neo-ovoidea	HKAS89025	China	-	MH508445	Cui et al., 2018
A. gymnopus	HKAS71618	China	MH486582	-	Cui et al., 2018
A. gymnopus	HKAS71618	China	-	MH508393	Cui et al., 2018
A. rhoadsii	DD97/13	USA	AF097391	-	Drehmel et al., 1999
A. curtipes	ASIS20105	Korea	KU139474	-	Data from GenBank
A. magniverrucata	RET 594-10	USA	KR919774	-	http://www.amanitaceae.org
A. magniverrucata	RET 594-5	USA	-	KR919765	http://www.amanitaceae.org
A. onusta	RET 297-3	USA	HQ539718	-	Wolfe et al., 2012
A. rhopalopus	BW_RET 386-3	USA	HQ539733	-	Wolfe et al., 2012
A. virgineoides	HKAS100518	China	MH486944	-	Cui et al., 2018
A. atkinsoniana	RET 301-1	USA	HQ539670	-	Wolfe et al., 2012
A. cf. *manginiana*	BZ_N11	Thailand	*KY747474	*KY747457	Thongbai et al., 2017
A. pallidochlorotica	HKAS77280	China	MH486730	-	Cui et al., 2018
A. preissii	PERTH 8690766	Australia	KY290654	-	Data from GenBank
A. sublutea	PSC 2401	Australia	HQ539749	-	Wolfe et al., 2012
A. oberwinklerana	HMJAU20940	China	-	MH508451	Cui et al., 2018
A. oberwinklerana	MHHNU 7114	China	FJ011684	-	Zhang et al., 2010
A. oberwinklerana	MHHNU 6826	China		FJ176727	Zhang et al., 2010
A. subcokeri	RET 097-3	USA	HQ539747	-	Wolfe et al., 2012
A. conicobulbosa	PSC 1368	Australia	HQ539683	-	Wolfe et al., 2012
A. effuse	PSC 2007	Australia	HQ539689	-	Wolfe et al., 2012
A. cokeri	BW_STF 090506-19	USA	HQ539682	-	Wolfe et al., 2012
A. costaricensis	RET 330-4 28S	USA	NG_057061	-	http://www.amanitaceae.org
A. subsolitaria	RET 327-4	USA	HQ539750	-	http://www.amanitaceae.org
A. pseudoporphyria	FB-30951(CBM)	Japan	-	*AB015702	Oda et al., 1999
A. pseudoporphyria	A4	China	-	*FJ441034	Data from GenBank

Table. (Continued).

A. fritillaria	A1	China	-	FJ441031	Data from GenBank
A. manginiana	SFC20140823-10	China	-	[*]KT779083	Loizides et al., 2018
A. olivovaginata	SUA138	Pakistan	MF491875	MF489722	This study
A. olivovaginata	SUA1438	Pakistan	MF491874	MF489724	This study
A. olivovaginata	SUA939	Pakistan	MF491873	MF489723	This study
A. ovalispora	HKAS96114	China	MH486723	-	Cui et al., 2018
A. ovalispora	HKAS79625	China	MH486722	MH508479	Cui et al., 2018
A. subovalispora	BZ2014_06	Thailand	MF461562	-	Thongbai et al., 2018
A. subovalispora	BZ2015_70	Thailand	-	MF461580	Thongbai et al., 2018
A. subovalispora	BZ2014_06	Thailand	MF461565	-	Thongbai et al., 2018
A. sp-GSM04	RET 375-9	USA	KX018802	KX018794	http://www.amanitaceae.org
A. rooseveltensis	RET 408-9	USA	MF621910	-	http://www.amanitaceae.org
A. goauldiorum	RET 368-3	USA	MK277538		http://www.amanitaceae.org
Amanita sp. (as *A. Alboflavescens*)	KA12-0970	Korea	KF021667	-	Kim et al., 2013
Amanita sp. (as *A. Alboflavescens*)	A7	China	-	FJ441037	Data from GenBank
A. aff. *vaginata*	TRTC150325	Thailand	KF877313	-	Sanchez-Ramirez et al., 2015
A. vaginata	LE<RUS>:9585	Russia	-	KM658298	Malysheva and Kovalenko, 2015
A. aff. *vaginata*	LE 296453	Russia	-	KM658296	Malysheva and Kovalenko, 2015
A. coprinopsoides	RET 236-10	USA	MK204469	-	http://www.amanitaceae.org
A. tenuifulva	HKAS87120	China	MH486929	-	Cui et al., 2018
A. punctate	RET 474-2	Australia	KU186804	-	http://www.amanitaceae.org
A. luteoparva	BZ2015_46	Thailand	MF461556	MF461575	Thongbai et al., 2018
A. simulans	TO PA151006	UK		KX834261	Vizzini et al., 2017
Amanita sp.	HKAS75475	China	MH486881	MH508606	Cui et al., 2018
A. orientifulva	HKAS97971	China	MH486707	-	Cui et al., 2018
A. orientifulva	KA12-1596	Korea	KF021680		Kim et al., 2013
A. umbrinolutea	HKAS94089	China	MH486935	-	Cui et al., 2018
A. carolinensis	RET 715-4	USA	MG937746	-	http://www.amanitaceae.org
A. cattaraugana	RET 694-9 28S	USA	KX261525	-	http://www.amanitaceae.org
A. battarrae	LE<RUS>:296458	Russia	KM658305	KM658290	Malysheva and Kovalenko, 2015
A. pachycolea	HKAS101423	China	MH486725	-	Cui et al., 2018
A. cinnamomea	BZ2015_48	Thailand	MF461557	MF461576	Thongbai et al., 2018
A. texasorora	RET 703-4	USA	KY435409		http://www.amanitaceae.org
A. pseudovaginata	HKAS70170	China	MH486792	-	Cui et al., 2018
A. pseudovaginata	A12	China	-	FJ441042	Zhang et al., 2010
A. pseudovaginata	LE<RUS>:216819	Russia	-	KM658285	Malysheva and Kovalenko, 2015
A. shennongjiana	HKAS75553	China	MH486862	-	Cui et al., 2018
A. constricta	BW_Mycoblitz IV_2	USA	HQ539684	-	Wolfe et al., 2012
A. brunneofuliginea	HKAS83536	China	MH486392	MH508268	Cui et al., 2018
A. submembranacea	AF3130	Thailand	MF461552	-	Thongbai et al., 2018
A. fulva	ASIS26398	Korea	KU139446	-	Data from GenBank
A. fulva	LE<RUS>:296456	Russia	-	KM658291	Malysheva and Kovalenko, 2015
A. olivaceofusca	HKAS98437	China	MH486693	MH508459	Cui et al., 2018

Table. (Continued).

A. olivaceofusca	HKAS80243	China	MH486689	-	Cui et al., 2018
A. rhacopus	RET 376-8	USA	-	KP224335	http://www.amanitaceae.org
A. glarea	SUA712	Pakistan	-	KY817312	Jabeen et al., 2017
A. populiphila	RET 119-1	USA	-	KP221308	http://www.amanitaceae.org
A. emodotrygon	MFM-219	Pakistan	MF491881	MF489730	This study
A. emodotrygon	SUA902	Pakistan	MF491880	MF489728	This study
A. emodotrygon	SUA601-2	Pakistan	MF491882	MF489729	This study
A. castellae	RET 664-8	USA	MH014783	-	http://www.amanitaceae.org
A. emodotrygon	CAL 1338	India	KX539266		Tibpromma et al., 2017
A. trygonion	RET 622-5	USA	KU186810	KU186809	http://www.amanitaceae.org
A. cf. *angustilamellata*	HKAS89451	China	MH486431	MH508292	Cui et al., 2018
A. penetratrix	RET 769-1	USA	MH836552	MH836563	http://www.amanitaceae.org
A. semiobruta	RET 691-1	USA	KY435401	KY435402	http://www.amanitaceae.org
A. flavidocerea	BZ2015_60	Thailand	F461560	MF461578	Thongbai et al., 2018
A. myrmeciae	RET 495-10	Australia	KU186806	-	http://www.amanitaceae.org
A. verrucosivolva	HKAS75608	China	MH486939	-	Cui et al., 2018
A. justice	RET 668-2	USA	MG928385	-	http://www.amanitaceae.org
A. williamsiae	RET 503-5	USA	MG981207	-	http://www.amanitaceae.org
A. penetrans	RET 696-4	USA	KX061536	-	http://www.amanitaceae.org
A. sp. H909	H909	Australia	-	GQ925403	Justo et al., 2010
A. albemarlensis	RET 690-3	USA	-	MK085521	http://www.amanitaceae.org
A. cingulata	HKAS:100640	China	-	MF952721	Liu et al., 2017
A. submembranacea	LE<RUS>:234914	Russia	-	KM658287	Malysheva and Kovalenko, 2015
A. crocea	LE<RUS>:234914	Russia	-	JQ912665	Malysheva and Kovalenko, 2015
A. pyramidata	HKAS87943	China	MH486795	MH508535	Cui et al., 2018
A. rubiginosa	HKAS52216	China	MH486817	MH508561	Cui et al., 2018
A. cinereoconia	BW_PSF	USA	HQ539677	-	Cui et al., 2018
A. cinereoradicata	HKAS 63641	China	NG_064564	-	Cui et al., 2018
Limacella glischra	VTGB505	USA	AY612843	-	Drehmel et al., 2008
Limacella illinita	VT8.9.96	USA	AF261439	-	Moncalvo et al., 2002
Limacella glischra	RET 540-6	USA	-	KT168219	http://www.amanitaceae.org
Limacella glischra	RET 502-8	USA	-	KT168221	http://www.amanitaceae.org

[*] Identified as a single new species, *A. caojizong* by Cui et al. (2018).

with a sampling frequency of 1000. Tracer 1.6 was used to check the effective sample size (ESS), and burn-in values were adjusted to achieve an overall ESS of ≥200. Maximum clade credibility tree (20% burn-in) was generated using TreeAnnotator 1.6.2 (Drummond and Rambaut, 2007). ML analyses were performed with RAxML-HPC2 on XCED (8.2.10) (Stamatakis, 2006), using 1000 bootstrap replicates and the default parameters as implemented on the CIPRES web portal. Fig Tree 1.4.2 was used for tree visualization, with additional tree annotation done through Adobe Illustrator CS6. Rapid bootstrap analysis/search for best-scoring ML tree (-f a) was configured. For the bootstrapping phase, the GTRCAT model was selected. One thousand rapid bootstrap replicates were run. Nodes were considered strongly supported when maximum likelihood bootstrap (MLB) were ≥70% and Bayesian posterior probability (BPP) were ≥0.95.

3. Results

Phylogenetic and morphological analysis of *Amanita* from the Shangla and Mansehra districts of Pakistan revealed that of the 3 taxa studied, 2 are new species, and 1 is a new record for the country. All 3 species are phylogenetically characterized and morphologically described below. The final aligned ITS dataset was 920 characters, and the aligned LSU dataset was 965 characters after being trimmed (trimming was done manually in MESQUITE 2.75). The results of phylogenetic analyses of the ITS and LSU datasets are summarized in Figures 2 and 3.

The ITS phylogram resolved in 2 clades, representing section *Vaginatae* (Fr.) Quél. (MLB 100% and BPP nonsignificant) and section *Roanokenses* Singer ex Singer (MLB 86% and BPP nonsignificant) as delimited by Cui et al. (2018) (Figure 2). Likewise, the LSU phylogram also resolved into sections *Vaginatae* (MLB 100% and BPP nonsignificant) and *Roanokenses* (MLB 84% and BPP nonsignificant) (Figure 3).

In the ITS phylogeny (Figure 2), *A. cinis* is resolved in section *Roanokenses* and is represented by 3 specimens: LAH-SUA733 (MF489726) = type, LAH-SUA752A

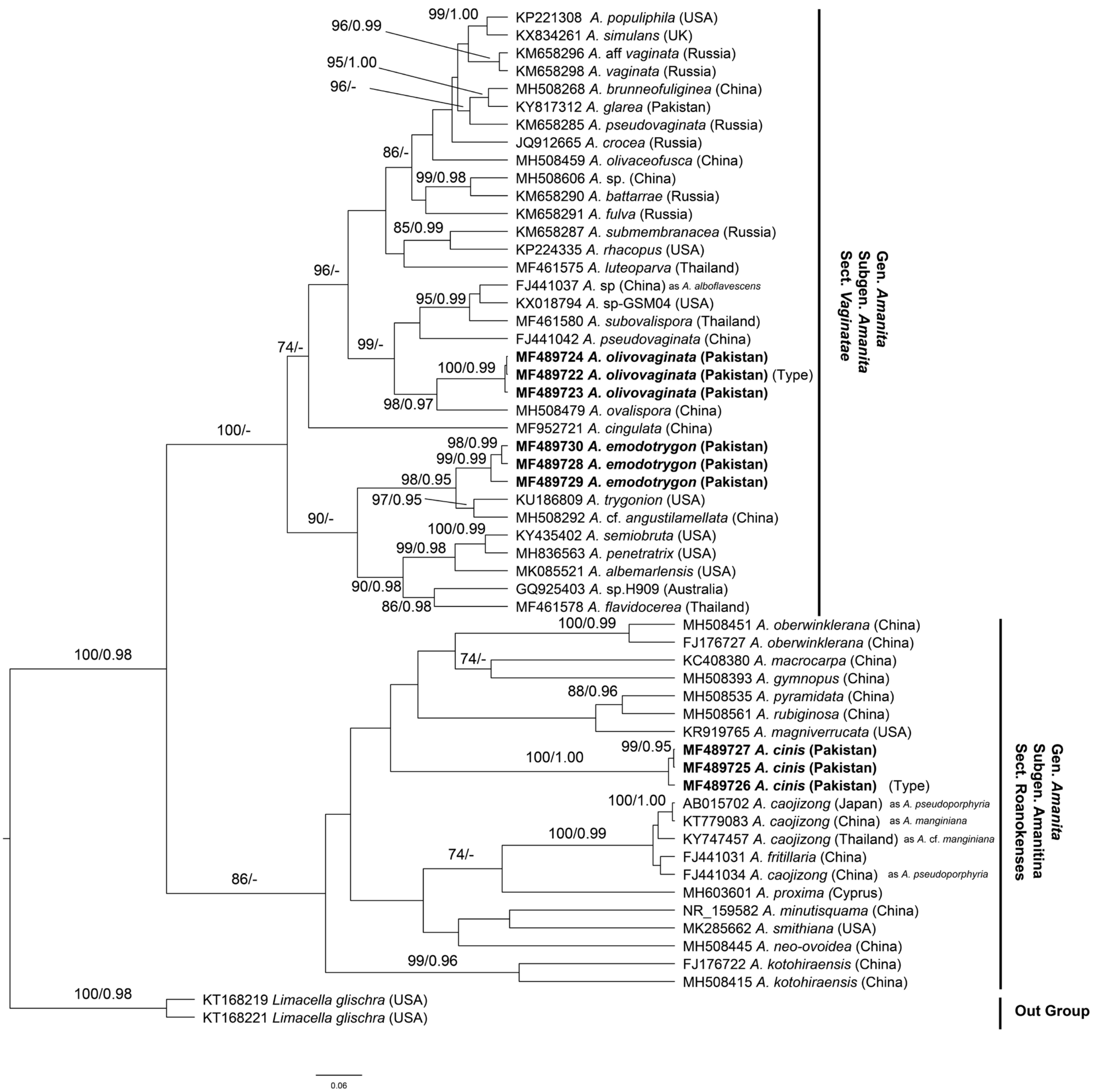

Figure 2. Phylogenetic Tree of *Amanita* species based on ITS sequence data from 57 nucleotide sequences. Sequences generated for this study are indicated in bold. Numbers above or below the branches indicate maximum likelihood bootstrap percentages followed by Bayesian posterior probabilities.

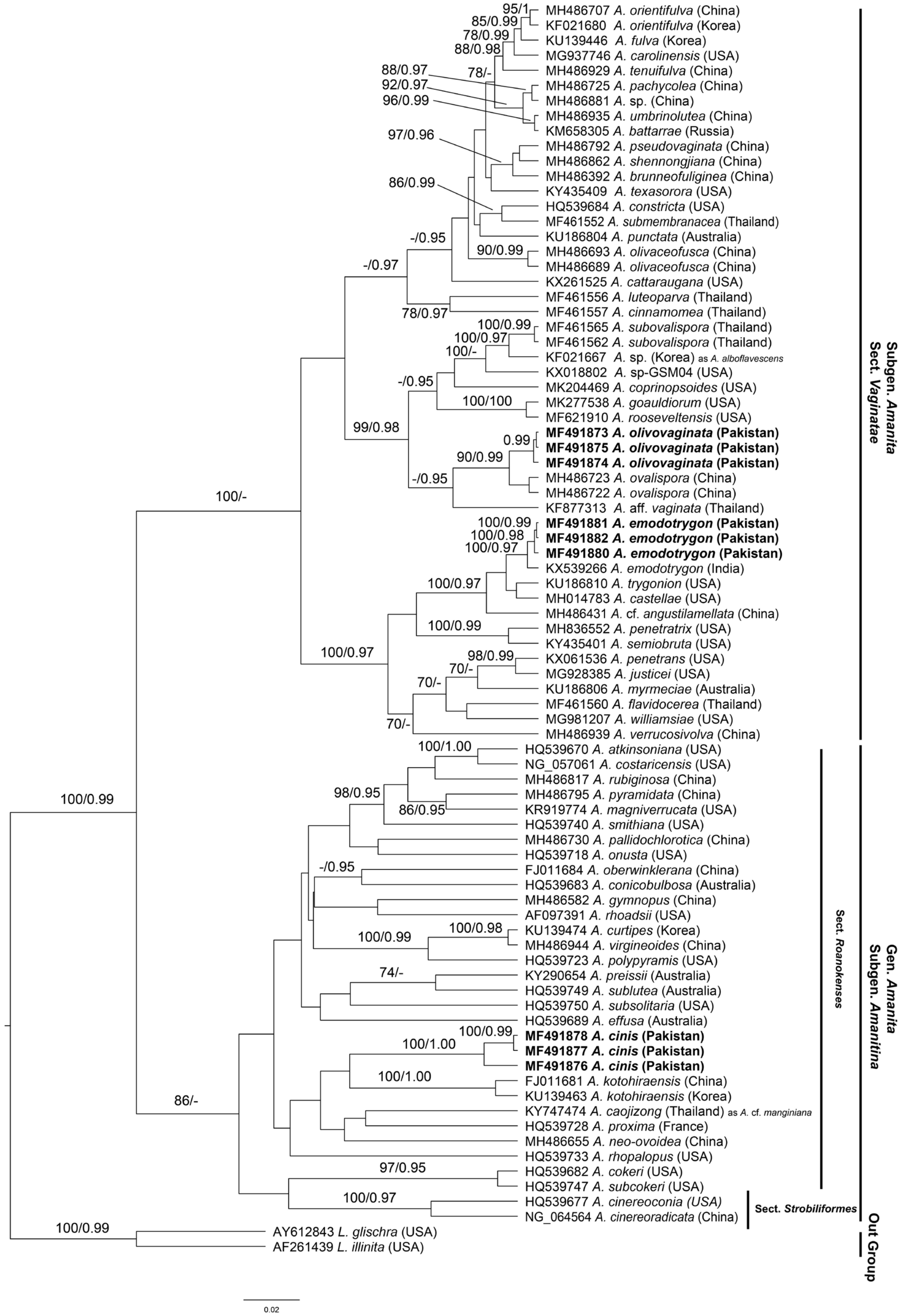

Figure 3. Phylogenetic Tree of *Amanita* species based on LSU sequence data of 83 nucleotide sequences. Sequences generated for this study are indicated in bold. Numbers above or below the branches indicate maximum likelihood bootstrap percentages followed by Bayesian posterior probabilities.

(MF489725), and LAH-SUA752B (MF489727), with 100% ML bootstrap support (MLB) and 0.99 Bayesian posterior probability (PP). They are resolved sister to a clade consisting of *A. magniverrucata* Thiers and Ammirati (KR919765, USA), *A. rubiginosa* Yang-Yang Cai et al. (MH50856, China), *A. pyramidata* Zhu L. Yang et al. (MH508535, China), *A. macrocarpa* W. Q. Deng et al. (KC408380, China), *A. gymnopus* Corner and Bas (MH508393, China), and *A. oberwinklerana* Zhu L. Yang and Yoshim. (MH508451, FJ176727, China). This relationship, however, is not statistically supported. *Amanita olivovaginata* is resolved in the section *Vaginatae* in the ITS phylogram with sequence from 3 specimens: LAH-SUA138 (MF489722) = type, LAH-SUA939 (MF489723), and LAH-SUA1438 (MF489724), with high statistical support (MLB 100% and BPP 0.99). It is resolved sister to *A. ovalispora* Boedijn (MH508479, China), with a high statistic support (98% MLB, 0.99 PP). Molecularly, the type of *A. olivovaginata* (MF489722) shares a nearly 90% sequence similarity to *A. ovalispora* (MH508479) based on a BLAST search. *Amanita emodotrygon* is also resolved in the section *Vaginatae* and is represented by 3 specimens: LAH-SUA601-2 (MF489729), LAH-SUA902 (MF489728), and LAH-MFM219 (MF489730) (100% MLB, 0.99 PP). They are resolved sister to a clade consisting of *A. trygonion* Tulloss et al. (KU186809, USA) and *A.* cf. *angustilamellata* (MH508292, China), with a high statistic support (98% MLB, 0.95 PP).

In the LSU phylogeny (Figure 3), *A. cinis* is resolved within the section *Roanokenses* with strong statistical support (100% MLB, 1.00 PP). It is resolved, unsupported, as sister to a clade including *A. kotohiraensis* Nagas. and Mitani (KU139463, Korea; FJ011681, China). Three specimens of *Amanita olivovaginata* form a clade within the section *Vaginatae* with strong support (100% MLB, 0.99 PP). It is resolved as sister to *A. ovalispora* (MH486723, MH486722, China), with 90% MLB and 0.99 PP. Finally, *A. emodotrygon* forms a clade within the section *Vaginatae*. It is sister to *A. emodotrygon* (KX539266) from India, with strong statistical support (100% MLB, 0.97 PP).

3.1. Taxonomy

Amanita cinis S. Ullah, A.W. Wilson, Tulloss & Khalid, sp. nov. (Figures 4 and 5)

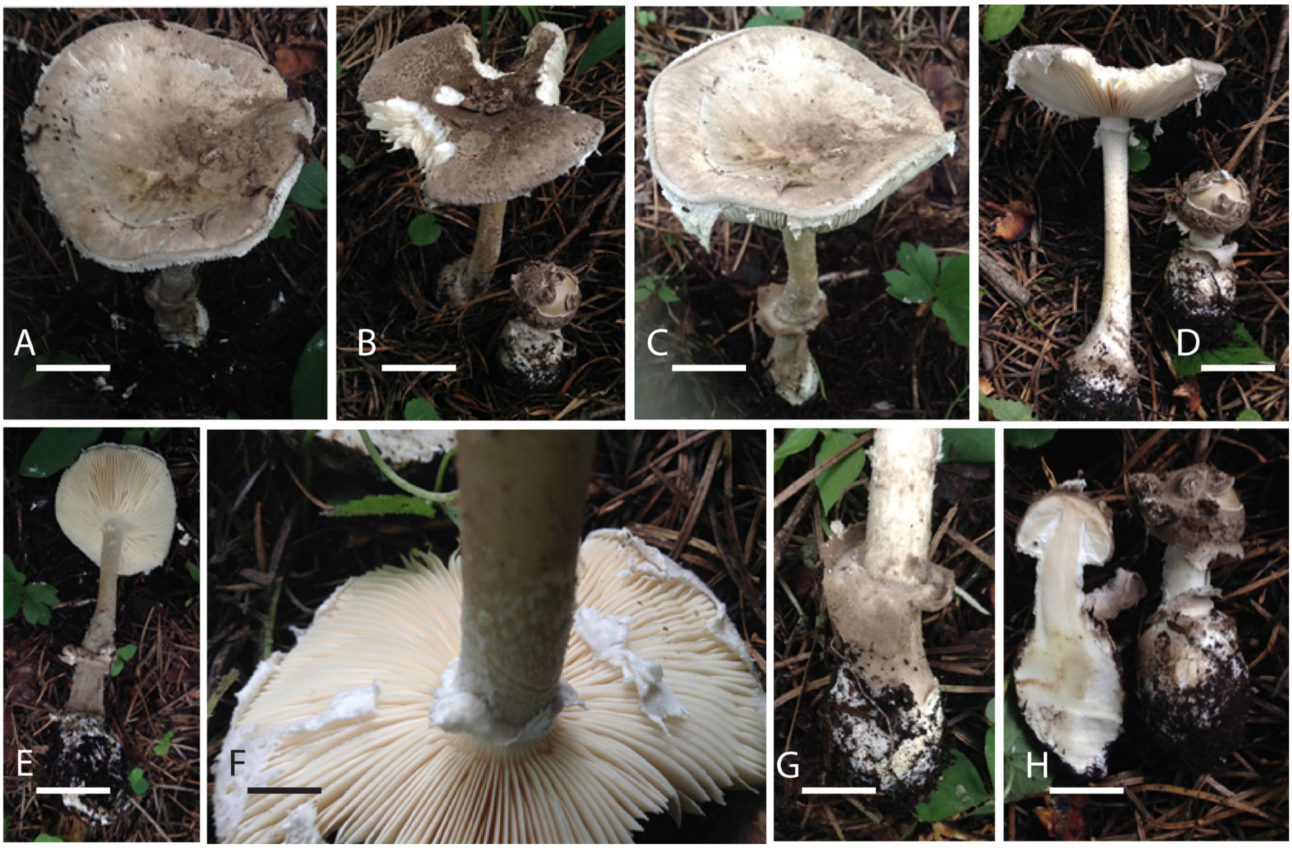

Figure 4. A–H. Morphological features of *Amanita cinis* (LAH-SUA733=A; HOLOTYPE): A–D. Basidiomata showing different features, E. Underside of basidioma showing position of stipe basal ring, F. Underside of pileus showing partial veil and gill attachment, G. Stipe showing basal ring above the bulb, H. Vertical section of Basidioma. Scale bar. A–C = 20 mm, D = 26 mm, E = 33 mm, F = 10 mm, G–H = 13 mm

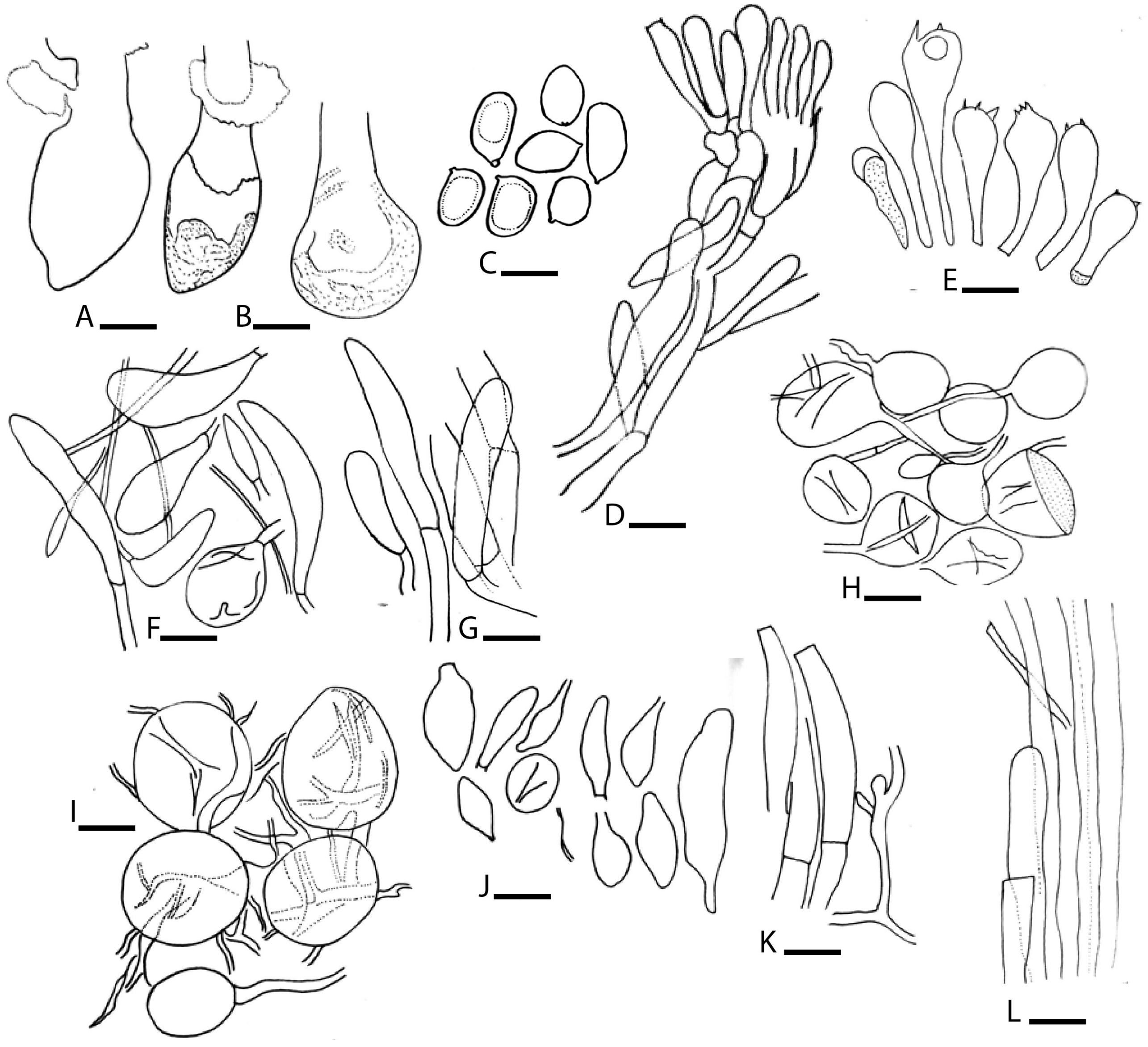

Figure 5. A–L. Morphological features of *A. cinis* (SUA733; HOLOTYPE): A. Vertical section of bulb, B. Shape of bulb with position of ring on lower stipe, C. Basidiospores, D–E. Hymenium and subhymenium, F. Pileipellis, G. Pileus context, H. Universal veil on pileus, I. Volval ring above the bulb, J. Elements of partial veil, K–L. Stipitipellis and stipe context. Scale Bars: A–B = 1 cm, C = 9 µm, D = 25 µm, E = 16 µm, F = 28 µm, G = 20 µm, H–I = 35 µm, I = 40 µm, J = 20 µm, K–L = 40 µm.

MycoBank No: MB 822040

Holotype: Pakistan, Khyber Pakhtunkhwa, Shangla District, Ajmir, Sham Burj, solitary on humus soil at 2400 m a.s.l. in mixed forest under *Abies pindrow*, September 01, 2013, Sadiq Ullah SUA733 (LAH-SUA733).

Etymology: "*cinis*" (ashes), refers to the color of universal veil remnants on the pileus surface.

Diagnosis: Pileus yellowish-brown and areolate, often completely covered by olive grayish ashen universal veil in the juvenile stage. At maturity the pileus has a well-formed cuticle, with large patches at the center that become light olive-brown pulverulence away from the center, pruinose to pulverulent at the periphery, and often lost with wind and rain. Stipe with small shredded apical annulus and a grayish, fugacious ring-like structure below. Basidiospores oblong or subcylindrical to rarely ellipsoid, (8.5–) 10–13 (–13.5) × (5.2–) 6–7.5 (–8.5) µm.

Description: PILEUS: 60–80 mm wide, originally pale yellow green (10Y 8/2) to grayish yellow green (10Y 7/2) to grayish yellowish brown (10YR 5/2) to light grayish olive (10Y 6/2), pale yellow green (10Y 8/2; 5GY 8/2) at margin, color and appearance dominantly ashen; plane to depressed to uplifted with straight to decurved margins, dull to tacky to subshiny, moist or dry, without umbo; pileipellis peeling easily when dry; *context* soft and fleshy when young, pure white, not changing when bruised, up to 9 mm thick over stipe, thinning toward margin; *margin* appendiculate, nonstriate; *universal veil* completely covering pileus surface at first, then as large flattened subpolygonal floccose ashen scales [light olive brown (2.5Y 5/2) to grayish yellowish brown (10YR 5/2)], sometimes becoming light olive brown (2.5Y 5/2) pulverulent and deciduous, sometimes with large scales remaining over disc in mature specimens, often turning light olive brown (2.5Y 5/6) when wet. LAMELLAE: sinuate, close, creamy in edge view, yellowish white to creamy in side view, 9–11 mm broad, convex, with gray-white edge fimbriate in tufts; *lamellulae* attenuate, ventricose, often evenly distributed, often present between every pair of gills, of diverse lengths. STIPE: 100–145 × 10–13 mm, pale yellow green (10Y 8/2; 5GY 9/2) to grayish greenish yellow (7.5Y 7/4) to light yellow green (5GY 9/4) to gray brown to dirty white to yellowish white, bruising light brown, cylindrical, flaring at apex, covered with whitish scales near apex, dirty white over central region, with gray remnants along lower region above bulb; *context* solid when young, yellowish cream, bruising slightly brownish to pale yellow green; *bulb* 24–25 × 18–24 mm, originally pure white, often decorated with grayish volval remnants, subglobose to ventricose; *partial veil* apical, cottony, shredded by the expansion of the pileus and may be lost entirely in some specimens, however, its remnants remain visible close to attachment point, white to dirty white to gray white, not changed on bruising; remnants of a well-developed *universal veil* absent at the stipe base, however, a grayish, ring-like structure is present up to 30 mm above the basal bulb of the lower stipe in mature specimens, present in young specimens just above the bulb, grayish, appearing similar to fine scales present on the pileus. In some specimens ashy remnants are visible on the stipe.

PILEIPELLIS: 175–250 µm thick, filamentous undifferentiated hyphae subradially arranged, hyaline, densely packed, 2–8 µm wide. PILEUS CONTEXT: filamentous undifferentiated hyphae 2.5–10 µm wide; acrophysalides plentiful, thin-walled, clavate to broadly clavate to cylindric, up to 130 × 32 µm; vascular hyphae 10 µm wide, rare. LAMELLA TRAMA: bilateral, divergent; w_{cs} = 48–76 µm; filamentous undifferentiated hyphae interwoven, 2.6–9 µm wide, with subhymenial base dominated by densely packed divergent filamentous undifferentiated hyphae 2.8–9 µm wide, vascular hyphae not observed. SUBHYMENIUM: $w_{st\text{-}near}$ = 80–95 µm; $w_{st\text{-}far}$ = 90–110 µm; branched, subglobose to ellipsoidal (8–19 × 8–14 µm) cylindric to clavate cells (23–52 × 9–12 µm) or uninflated hyphal segments, with such elements arranged approximately perpendicular to central stratum, mostly 4–5 layers. BASIDIA: (29–) 34–53.7 × 7.5–10 µm, 4- and (frequently) 2-sterigmate, with sterigmata up to 4.9 × 1.5 µm; clamp connections absent. UNIVERSAL VEIL: *On pileus:* filamentous undifferentiated hyphae 2–5.8 µm wide; inflated cells dominating, globose to subglobose to ellipsoid to convex to pyriform to sphaeropedunculate 23–56 × 23–48 µm, very infrequently elongate to narrow cylindrical (9 × 44 µm, collapsed and partially gelatinized); vascular hyphae not observed. *On stipe base (largely above basal bulb)*: filamentous undifferentiated hyphae 2.3–7.8 µm wide, branching, singly or in fascicles, common, more frequent than on pileus; inflated cells plentiful, similar in shape to those on pileus but with a well-developed stalk, mostly sphaeropedunculate, 37–66 × 30–62 µm; vascular hyphae not observed.

STIPE CONTEXT: longitudinally acrophysalidic; filamentous undifferentiated hyphae 4–7.5 µm wide, branching; acrophysalides plentiful to dominant up to 20–30 µm wide; vascular hyphae up to 22 µm wide, occasionally branching, unevenly distributed. PARTIAL VEIL: inflated cells dominating, cylindrical to broadly clavate to narrowly clavate to pyriform, 23–70 × 9–21; filamentous, undifferentiated hyphae 1.3–5.5 µm wide, branching, singly and in fascicles.

BASIDIOSPORES: [160/3/3] (8.5–) 10–13 (–13.5) × (5.2–) 6–7.5 (–8.5) µm (**L** = 10.6–13, **L**′ = 11 µm, **W** = 5.5–7.5, **W**′ = 7.1 µm), Q = 1.23–1.94, **Q** = 1.34–2.0 µm (**Q**′ = 1.54 µm), oblong or subcylindrical, rarely ellipsoidal, hyaline, thin-walled, smooth, amyloid; *apiculus* sublateral, small, truncate to conic; *contents* monoguttulate.

Known distribution: In *Abies* forests in Hindu-Kush and Himalaya regions of Pakistan between 2400 m–2600 m a.s.l.

Additional material examined: Pakistan, Khyber Pakhtunkhwa, Shangla District, Takht Burj, on humus dark soil at 2600 m a.s.l., in mixed coniferous forest under *Abies pindrow*, September 01, 2014 S. Ullah SUA752A (LAH-SUA752A); Takht, 2600 m a.s.l., on soil under *Abies pindrow*, September 01, 2015 Sadiq Ullah SUA752B (LAH-SUA752B).

Comments: ITS phylogenetic analysis (Figure 2) indicates that *A. cinis* is related to *A. magniverrucata* (KR919765, USA), *A. rubiginosa* (MH508561, China), *A. pyramidata* (MH508535, China), *A. macrocarpa* (KC408380, China), *A. gymnopus* (MH508393, China), *A. oberwinklerana* (MH508451, FJ176727, China), while on the LSU phylogram (Figure 3) it is related to *A. kotohiraensis* (KU139463, Korea; FJ011681, China), *A. neoovoidea* (MH486655, China), *A. proxima* (HQ535728, France), *A.* cf. *manginiana* (KY747474, Thailand [currently known as *A. caojizong* by Cui et al., 2018]), and *A. oberwinklerana* (FJ011684, China). However, *A. magniverrucata* has a slender basidioma, a relatively pale pileus, volval remnants on the pileus that are at first a thick and rather smooth covering over the entire pileus, becoming areolate and later appearing as larger conspicuous pyramidal warts, and relatively small narrower basidiospores (8.0–12.6 × 5.8–8.0 m) (Tulloss, 2009). *Amanita rubiginosa* has verrucose to pyramidal volval remnants on pileus, often white at apex; volval remnants on stipe base forming as verrucae, basal bulb often with a reddish tinge, and smaller basidiospores 8.0–10.0 × 6.5–8 (Cui et al., 2018). *Amanita pyramidata* has pyramidal to verrucose volval remnants on pileus which is 1–3 mm in height and width, with margin sometimes pinkish tinged basal bulb covered with verrucose to conical recurved squamules often in belts and relatively smaller but broader basidiospores (9.0–11.0 × 9 7.5–9.5, Q = 1.1–1.27, Qm = 1.18 ± 0.06). *Amanita macrocarpa* W. Q. Deng et al. has a larger basidioma with a pileus ca. 15–24 cm in diam., pyramidal volval remnants on the pileus, verrucose, brownish to yellowish volval remnants on the stipe base, and relatively small and narrower basidiospores (7.0–9.0 × 5.0–6.0 μm [Deng et al., 2014; Cui et al., 2018]). *Amanita gymnopus* has small basidiospores 6.0–8.5 × 5.5–7.5 μm and often lacks volval remnants on stipe base. *Amanita oberwinklerana* has a white pileus, limbate volva, lacking volval remnants on pileus or sometimes with 1–3 large white patches, a white stipe which is covered with fibrous to tomentose white squamules, annulus that is subapical to submedian and ellipsoid to broadly ellipsoidal small spores 8.0–10.5 × 6.0–8.0 μm (Cui et al., 2018). *Amanita neoovoidea* has white to off-white cap, limbate membranous volva, and smaller broadly ellipsoid to ellipsoid spores 6.8–9.8 × 4.8–6.5 μm (Yang, 1997). *Amanita kotohiraensis* has a white pileus, volval remnants on pileus felted to patchy, white stipe covered with minute, white squamules, and broadly ellipsoidal to ellipsoidal small basidiospores 7.5–9.5 × 5.0–6.5 μm (Nagasawa and Mitani, 2000; Cui et al., 2018).

In our phylogenetic analysis, 4 ITS sequences of section *Roanokenses,* AB015702 (*A. pseudoporphyria,* Japan), KT779083 (*A. manginiana,* Republic of Korea), KY747457 (*A.* cf. *manginiana,* Thailand), FJ441034 (*A. pseudoporphyria*), and 1 LSU sequence KY747474 (*A.* cf. *manginiana,* Thailand), were recently identified as a single new species *A. caojizong* by Cui et al., (2018). *Amanita caojizong* has large, brownish gray to dark gray pilei, with innate, dark gray, radiating fibrils, sometimes umbonate at the center; volval remnants on pileus absent or sometimes with retained white patches; white stipe, covered with fibrous to pulverulent white squamules, volva limbate and membranous, annulus large and fugacious; spores small broadly ellipsoidal to ellipsoidal 6.0–8.0 (–9.0) 9 4.5–6.5 μm, Q = 1.16–1.57 μm (Cui et al., 2018). *Amanita proxima* (HQ539728) has a membranous partial veil, an ochraceous to reddish brown, membranous volva; a whitish to ivory cap; ochraceous to reddish brown veil, and ellipsoidal to elongate spores measuring (8.2–) 8.9–12.4 (–17.5) × (5.0–) 5.5–7.2 (–9.9) μm (Dumée, 1916). *Amanita nana* is the only other species of *Amanita* sect. *Lepidella* reported from Pakistan (Ahmad, 1956; Bas, 1969); however, it falls in the group of nonmycorrhizal amanitas with their distinctive universal veil and white cap (Bas, 1969).

Amanita olivovaginata S. Ullah, Tulloss & Khalid, sp. nov. (Figures 6 and 7)

MycoBank No: MB 822039

Holotype: Pakistan, Khyber Pakhtunkhwa, Shangla District, Dherai, 1800 m a.s.l., in sandy to loamy soil under *Pinus roxburghii* Sarg, August 15, 2014, Sadiq Ullah, SUA 138 (LAH-SUA138).

Etymology: Named "*olivovaginata*" because of its "light olive brown to light grayish olive" pileal color and its placement in *Amanita* sect. *Vaginatae*.

Diagnosis: Pileus surface light olive brown to light grayish olive, depressed to lightly depressed at disc, striate to sulcate margins, thin trama, fibrillose to floccose stipe, saccate volva, eroded lamellae, Basidia 2-sterigmate and basidiospores 8.5–11.0 × 7.0–9.0 μm subglobose to broadly ellipsoidal to ellipsoidal.

Description: PILEUS 50–100 μm wide, light olive brown (2.5Y 5/2) to light grayish olive (10Y 5/2) at disc, dark grayish yellow (5Y 6/4) to light grayish olive (10Y 6/2) away from the disc, and finally, light brown pale yellow-green (10Y 8/2) to pale yellow green (5GY 8/2) toward the margins, depressed to slightly depressed, smooth to lightly fibrillose, dull, dry, without umbo; context very thin, white, up to 2 mm thick above stipe, thinning to membrane at margin; margin striate to sulcate, (0.5–0.7R), decurved, nonappendiculate; universal veil not observed on pileus surface; LAMELLAE: free, subdistant, up to 7 mm broad, usually broader near margin and narrowing toward stipe, with pure white edges, eroded; lamellulae present, regularly spaced, sinuate at free end, of diverse lengths. STIPE: 100–120 × 6–11 mm, often flexuous, sometime narrowing upward and downward, flaring at apex, punctate, with pure white small scales; exannulate; universal veil as saccate membranous volva, 20–40 × 8–10 mm, fibrous, persistent, bright white to off-white on exterior surface, not changed with handling, off-white on interior surface.

PILEIPELLIS: 75–150 μm thick, filamentous undifferentiated hyphae 2–8 μm wide, PILEUS CONTEXT: filamentous undifferentiated hyphae 2.5–10 μm wide; acrophysalides plentiful, thin-walled, clavate to broadly clavate to cylindrical, up to 125 × 35 μm; vascular hyphae 10 μm wide, rare. LAMELLA TRAMA: bilateral, divergent; w_{cs} = 22–50 μm; central stratum comprising of filamentous undifferentiated hyphae 3–8 μm wide and

Figure 6: A–K. Morphological features of *A. olivavaginata* (SUA138=A, HOLOTYPE): A–E. Basidiomata showing sulcate to plicate margins; F. Pileus at underside showing gills attachment, eroded margins, and thin trama; G–H. Basidiomata showing crowded pure white scales on stipe; I–K. Basidiomata showing volva and pileus color. Scale bar: A = 20 mm, B = 12 mm, C = 20 mm, D = 3.5 mm, E–G = 18 mm, H–I = 7.3 mm, J–K = 2 mm

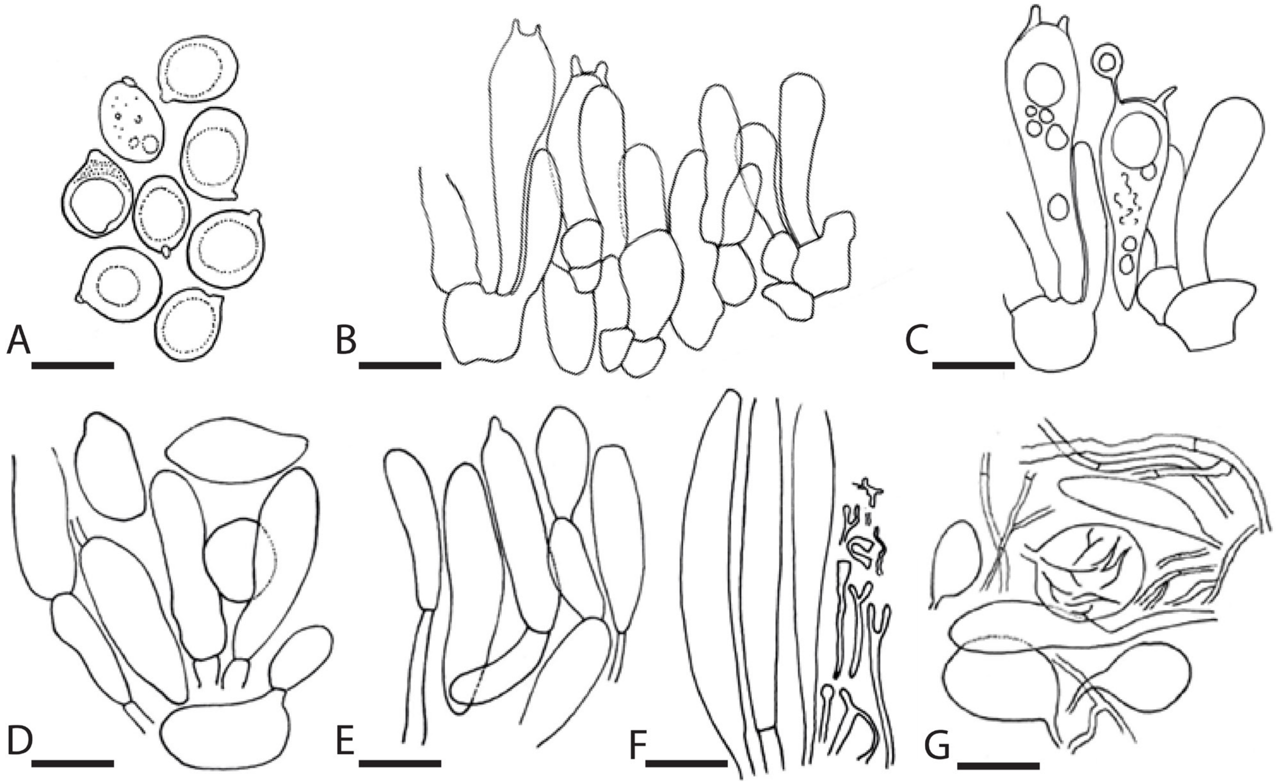

Figure 7: A–G. Micromorphological features of *A. olivovaginata* (SUA138=A, HOLOTYPE): A. Basidiospores, B–C. Hymenium and subhymenium, D. Trama cells of Lamellae, E. Pileipellis, F. Stipitipellis, G. Volval elements Scale bar: A = 9 µm, B–C = 13 µm, D = 30 µm, E = 33 µm, F = 40 µm, G = 45 µm

oblong to ellipsoid to fusiform to broadly cylindrical to pyriform to clavate inflated cells 32–80 (–108) × 10–32 (–64) µm, occasionally with globular cells 12–20 × 8.8–14 µm. SUBHYMENIUM: wst-near = 60–100 µm; wst-far = 90–130 µm; basidia arising from irregular subglobose to elongated cells of subhymenium measuring 9–19 × 7–13 µm. BASIDIA: (32–) 34–45 (–52) × (9.3–) 10–13 (–13.2) µm clavate, 2-sterigmate, with sterigmata up to 5.5 × 1.5 µm; clamp connections absent. UNIVERSAL VEIL: On pileus: absent; stipe base surface layer composed of longitudinally filamentous hyphae, abundant and dominant, 2–8 µm broad, inflated cells scarce, mostly subglobose 35–75 × 35–55 µm, rarely elongated cylindrical, 40–130 × 19–35 µm, colorless, thin-walled, mostly terminal; vascular hyphae not observed. Inner layer composed of dense, hyaline, cylindrical hyphae, 3–10 µm broad,: filamentous hyphae dominant; inflated cells scarce, mostly subglobose, 40–80 × 33–52 µm very rarely ellipsoid to fusiform to cylindrical, up to 40–130 × 19–35 µm, vascular hyphae not observed. STIPE CONTEXT: longitudinally acrophysalidic, filamentous, undifferentiated hyphae 4–7.5 µm wide, branching, acrophysalides plentiful to dominant, up to 8–20 µm wide.

BASIDIOSPORES: [100/3/3] (8.0–) 8.5–11.0 (–11.3) × (7.0––9.0 (–9.5) µm [**L** = 9–10, **L′** = 9.9 µm, **W** = 7.5–8.2, **W′** = 7.8 µm), Q = 1.08–1.34, **Q** = 1.19–1.24 µm (**Q′** = 1.21 µm], subglobose to broadly ellipsoid to ellipsoid, inamyloid; contents mostly monoguttulate, occasionally without guttule and then with small granules; apiculus short, truncate conic.

Known distribution: In Pine forests in Hindu-Kush and Himalaya regions of Pakistan 1800 m–1900 m a.s.l.

Additional specimens examined: Pakistan, Khyber Pakhtunkhwa, Shangla District, Chawga forest, 1900 m a.s.l., on loamy to sandy soil under *Pinus roxburghii*, September 01, 2015, Sadiq Ullah SUA 1438 (LAH-SUA1438); Mansehra District, on the border of Mansehra and Bataagram districts, 1900 m a.s.l., on sandy soil under *Pinus roxberghii*, August, 05 2015, Sadiq Ullah SUA939 (LAH-SUA939).

Comments: *Amanita olivovaginata* is characterized by its light olive-brown to light grayish olive pileus, thin trama, striate to sulcate margins, fibrillose to floccose stipe, saccate volva, eroded lamellae, 2-spored basidia, scarce inflated cells in the volval remnants on the stipe base, subglobose to broadly ellipsoid to ellipsoid basidiospores

8.5–11.0 × 7.1–9.0, and is found in association with *Pinus roxberghii*.

Phylogenetically, *A. olivovaginata* is related to *A. ovalispora, A. pseudovaginata, A. subovalispora* Thongbai et al., and *Amanita* sp. (FJ441037). Morphologically, *A. olivovaginata* is similar to *A. ovalispora* by having a thin trama, exannulate appearance, striate margins, fibrillose to floccose stipe and saccate volva (Yang, 1997, 2001, 2015). However, *A. ovalispora* has a gray to dull gray cap, convex to planoconvex pileus, sometimes slightly umbonate and often campanulate at initial stages, crowded lamellae, smooth edges, 4-spored basidia (33–50 × 12–15 µm) and large ovoid-ellipsoidal or broadly ellipsoidal to ellipsoidal basidiospores (8.0–) 9.0–11.0 (–12.0) × (7.0–) 7.5–9.0 (–10.0) µm, Q = 1.3 ± 0.13] (Yang, 1997, 2001, 2015; Cui et al., 2018). *Amanita pseudovaginata* is grayish sometimes with a brownish tinge, and occasionally nearly white with a smooth stipe. Spore size in *A. pseudovaginata* is also larger, 9.5–12.5 (–14.0) × (7.0–) 8.0–10.5. The pileus of *A. vaginata* lacks an umbo, is grayish with a striate margin, crowded lamellae with entire margins, and larger globose to subglobose basidiospores measuring 10.0–13.5 (–16.5) × (8.5–) 9.2–12.2 µm (Tulloss et al., 2001). *Amanita subovalispora* has dark gray pileus, darker grayish black at center, nearly free to adnexed lamellae, mostly 4-spored basidia, broadly ellipsoidal to ellipsoidal longer basidiospores (8.9–11.7 × 7.3–8.8) µm, abundant inflated cells in the volval remnants on stipe base and is associated with mixed Dipterocarpaceae–Fagaceae forest (Thongbai et al., 2018). Morphologically *A. olivovaginata* is similar to *A. olivaceofusca* Cui et al. in appearance. However, the latter species possess brown to dark brown pileus with olive tinge, crowded lamellae, 4-spored basidia, abundant inflated cells in the inner surface of volval remnants on stipe base and large basidiospores (9.5–) 10.5–13.0 (– 15.0) × (8.0–) 8.5–10.0 (–11.5) µm (Cui et al., 2018).

Amanita emodotrygon Mehmood et al., in Fungal Diversity 83: 157 (2017) (Figures 8 and 9)

Description: PILEUS: 35–80 mm wide, parabolic to convex to plano-convex, glabrous, shiny, dry, slightly umbonate, pileipellis peeled at some points; margins nonappendiculate, sulcate to plicate with distinct regular veins and corresponding grooves, sometime split when mature; grayish yellowish brown (10YR 5/2) at disc then become light grayish brown and finally pale yellow green (10Y 9/2) to grayish yellow brown at edges; universal veil on pileus absent; context up to 8 mm over stipe, texture soft, and fibrous, first thinning slowly then rapidly toward margin, membranous at margin, white, not changed on bruising. LAMELLAE: sinuate, close, yellowish white to creamy in side view, gray-white at edges, 8–15 mm broad; lamellulae unevenly distributed, truncate, connected only at margins.

STIPE: 90–220 × 9–13 mm, central, subcylindrical, tapering upward, lightly striated at apex, covered with white to dirty white or grayish membranous cuticle that peels easily, sometime the upper half densely covered with small white to whitish granular membranous remains; white to dirty white to gray brown to yellowish white, not bruising; context white to yellowish white, not bruising, hollow; partial veil absent; volva saccate, persistent, membranous, 20–30 × 18–22 mm, white, often with rusty brown coloration, persistent, membranous, 20–30 × 18–22 mm.

PILEIPELLIS: 90–120 µm thick, comprised of branched filamentous hyphae 3–13 µm with elongated, clavate, and cylindrical terminal elements 10.7–53 × 8.8–13.2 µm. PILEUS CONTEXT: filamentous undifferentiated hyphae 2–10 µm wide; acrophysalides plentiful, clavate to broadly clavate to cylindrical, up to 131 × 29 µm; vascular hyphae 12 µm wide. LAMELLAR TRAMA: bilateral, divergent; w_{cs} = 65–85 µm; central stratum comprising of interwoven filamentous undifferentiated hyphae 3–12 µm wide and globular to subglobular or irregular cells 7–14 × 6–10.8 µm. SUBHYMENIUM: W_{st}-near = 34–66 µm; W_{st}-far = 55–110 µm; basidia arising mostly from inflated to irregular cells (up to 9–14 × 6–10 µm wide). BASIDIA: (35–) 37–53.7 × 8.5–14.5 µm, 2–4 spored, sterigmata up to 3.7 µm long, without basal clamp connections. UNIVERSAL VEIL of pileus not observed; of stipe base hyphae dominated by septate, branched filamentous undifferentiated hyphae, 4–10 µm wide, slightly thick-walled, subglobular cells 41–85 × 38–64 µm, and clavate cells 40–90 × 15–40 µm. STIPITIPELLIS: composed of 2 types of hyphae, the smaller up to 7 µm wide and the larger up to 20 µm wide. STIPE CONTEXT: longitudinally acrophysalidic; filamentous, undifferentiated hyphae 4–7.5 µm wide, acrophysalides dominant up to 28 × 180 µm wide. PARTIAL VEIL: absent.

BASIDIOSPORES [180/5/3] (7.4–) 8–13.3 (–14.3) × (6.7–) 7–11.5 (–11.8) µm (**L** = 10–12.8, **L′** = 11 µm, **W** = 7.5–11, **W′** = 8.8 µm), Q = 1.01–1.12, **Q** = 1.01–1.14 µm (**Q′** = 1.14 µm), globose to subglobose or broadly ellipsoid, hyaline often with 1 large guttule with gray brown walls, inamyloid; apiculus up to 2 µm long.

Known distribution: In pine forests in Hindu-Kush and Himalaya regions of Pakistan and India between 1500 m–1900 m a.s.l.

Material examined: Pakistan, Khyber Pakhtunkhwa, Shangla District, Sanela, in sandy soil under *Pinus roxburghii* at 1700 m asl, August 25, 2014 Sadiq Ullah SUA601-2 (LAH-SUA601-2); Shangla District, buneerwall, in sandy soil in pure forest of *Pinus roxberghii* at 1500 m a.s.l., August 20, 2015 Sadiq Ullah SUA902 (LAH-SUA902); District Mansehra, Oghi, Khabbal Paein, solitary on ground along with *Pinus roxburghii* Sarg., at 1905 m a.s.l., August 2010. Muhammad Fiaz LAH-MFM–219.

Figure 8. A–G. Morphological features of *A. emodotrygon*: A–C. Basidiomata showing different features, D. Lamellae showing dentate eroded margins, E. Pileus underside, F–G. Basidiomata showing margins and color. Scale bar. A–B = 23 mm, C = 40 mm, D = 13 mm, E–G = 20 mm

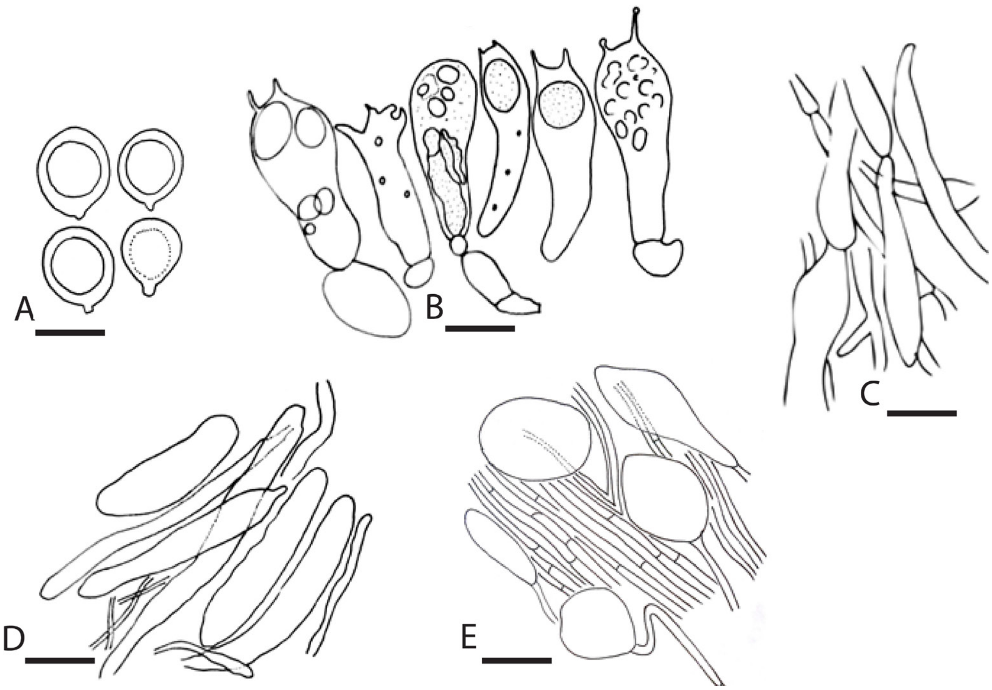

Figure 9. A–G. Micromorphological features of *A. emodotrygon* (SUA601-2): A. Basidiospores, B. Basidia, C. Pileipellis, D. Stipitipellis, E. Volval elements Scale bar: A = 10 µm, B = 15 µm, C = 16 µm, D = 28 µm, E = 30 µm.

Comments: *Amanita emodotrygon* was described from India and is characterized by convex to campanulate pileus, thick context thinning toward margin, membranous margin with distinct regular veins or striations and corresponding grooves, free and crowded lamellae 6 mm broad, saccate volva with many olive-brown spots on exterior surface, not bruising when damaged, and globose to subglobose basidiospores 8.8–13.5 × 8–13 µm with Q = 1.05–1.11 (Tibpromma et al., 2017). However, collections from Pakistan have parabolic to convex to plano-convex pileus, margins sometime split, lamellae up to 12 mm broad with eroded edges, and spores 8–14 × 7–11.5 µm (Q = 1.01 –1.14 µm). These discrepancies are clearly part of the variability of the species.

Acknowledgments

The work was financially supported by the International Research Support Initiative Program (IRSIP) of Higher Education Commission (HEC) Pakistan. Molecular lab work was performed in the Harris Family Foundation Plant Genetics Laboratory in the Department of Plant Biology and Conservation at The Chicago Botanic Garden, as well as the Pritzker Laboratory at the Field Museum of Natural History, Chicago, IL, USA.

References

Ahmad S (1956). Fungi of West Pakistan. Monographs. Biological Society of Pakistan 1: 1-126.

Bas C (1969). Morphology and subdivision of *Amanita* and a monograph on its section *Lepidella*. Persoonia 5: 285-579.

Champion GH, Seth SK, Khattak GM (1965). Forest types of Pakistan. Pakistan Forest Institute, Peshawar. 238.

Chen ZH, Yang ZL, Zhang SG (2001). Three noteworthy *Amanita* of subgenus *Lepidella* from China. Mycotaxon 79: 275-284.

Chen ZH (2014). New advances in researches on poisonous mushrooms since 2000 Mycosystema 33: 493-516.

Cui YY, Cai Q, Tang LP, Liu JW, Yang ZL (2018). The family Amanitaceae: molecular phylogeny, higher-rank taxonomy and the species in China. Fungal Diversity 91: 5-230. doi: 10.1007/s13225-018-0405-9

Deng W-Q, Li T-H, Li P, Yang ZL (2014). A new species of *Amanita* section *Lepidella* from South China. Mycological Progress 13: 211-217. doi: 10.1007/s11557-013-0906-6

Drehmel D, Moncalvo JM, Vilgalys R (1999). Molecular phylogeny of *Amanita* based on large-subunit ribosomal DNA sequences: implications for taxonomy and character evolution. Mycologia 91: 610-618.

Drummond AJ, Rambaut A (2007). BEAST: Bayesian evolutionary analysis by sampling trees. BMC Evolutionary Biology 7(1): 214. doi: 10.1186/1471-2148-7-214

Dumée, P (1916). Notes de mycologie pratique. 4. Note sur une amanite voisine d'*Amanita ovoidea, Amanita proxima* Dumée nom. sp. Bulletin de la Société Mycologique de France. 32: 83 (in French).

Edgar R (2004). MUSCLE: multiple sequence alignment with high accuracy and high throughput. Nucleic Acids Research 32(5): 1792-1797. doi:10.1093/nar/gkh340

Endo N, Fangfuk W, Kodaira M, Sakuma D, Hadano E et al. (2017). Reevaluation of Japanese *Amanita* section *Caesareae* species with yellow and brown pileus with descriptions of *Amanita kitamagotake* and *A. chatamagotake* spp. nov. Mycoscience 58: 457-471.

Fiaz M (2013). Species Diversity of Basidiomycetes of District Mansehra, PhD, Department of Botany, Hazara University Mansehra, Khyber Pakhtunkhwa, Pakistan.

Gardes M, Bruns TD (1993). ITS primers with enhanced specificity for basidiomycetes application to the identification of mycorrhizae rusts. Molecular Ecology 2: 113-118.

Gernhard T (2008). The conditioned reconstructed process. Journal of Theoretical Biology 253(4): 769-778. doi: 10.1016/j.jtbi.2008.04.005

Justo A, Morgenstern I, Hallen-Adams HE, Hibbett DS (2010). Convergent evolution of sequestrate forms in *Amanita* under Mediterranean climate conditions. Mycologia 102 (3): 675-688.

Jabeen S, Kiran M, Ullah S, Wilson AW, Mueller GM et al. (2017). *Amanita glarea*, a ringless new species in section *Vaginatae* from Pakistan. Phytotaxa, 306: 135-145.

Jie C, Zhang Z, Di L, Fei L, Xia C et al. (2009). ITS sequence analysis of 8 *Amanita* species from Tibeta and Yunnan. Journal of Yunnan University Natural Sciences Edition 31(1): 90-96.

Kim CS, Jo JW, Kwag YN, Oh J, Shrestha B et al. (2013). Four newly recorded *Amanita* species in Korea: *Amanita* sect. *Amanita* and sect. *Vaginatae*. Mycobiology 41 (3): 131-138.

Kiran M, Khan J, Naseer A, Sher H, Khalid AN (2017). *Amanita pallidorosea* in Pakistan and its ectomycorrhizal association with *Quercus oblongata*. Mycotaxon 132: 799-811.

Liu J-W, Cai Q, Coi Y-Y, Yang ZL (2017). *Amanita cingulata*, a new annulate species of *Amanita* sect. *Vaginatae* from subtropical China Phytotaxa 326 (1): 41-53. doi: 10.11646/phytotaxa.326.1.3

Loizides M, Bellanger J-M, Yiangou Y, Moreau P-A (2018). Preliminary phylogenetic investigations into the genus *Amanita* (Agaricales) in Cyprus, with a review of previous records and poisoning incidents. Documents mycologiques XXXVII, 201-218.

Moncalvo JM, Vilgalys R, Redhead SA, Johnson JE, James TY et al. (2002). One hundred seventeen clades of euagarics. Molecular Phylogenetics and Evolution 23: 357-400.

Maddison DR, Maddison WP (2005). MacClade 4, 4.07 ed. Massachusetts, USA: Sinauer Associates, Inc. Publishers Sunderland, 1-492.

Malysheva EF, Kovalenko AE (2015). Fungi of the Russian Far East. 4. Contribution to the study of *Amanita* sect. *Vaginatae* in the central Sikhote-Alin. Mikologiya i Fitopatologiya l49: 151-163.

Moncalvo JM, Drehmel D, Vilgalys R (2000). Variation in modes and rates of evolution in nuclear and mitochondrial ribosomal DNA in the mushroom genus *Amanita* (Agaricales, Basidiomycota): phylogenetic implications. Molecular Phylogenetics and Evolution 16 (1): 48-63.

Munsell AH (1975). Munsell soil color charts. Baltimore, MD, USA.

Nagasawa E, Hongo T (1984). New taxa of *Amanita*: Three new species and one new from western Japan. Transactions of the Mycological Society of Japan 25: 367-376.

Nagasawa E, Mitani S (2000). A new species of *Amanita* section *Lepidella* from Japan. Memoirs of the National Science Museum, Tokyo 32: 93-97.

Niazi AR, Iqbal SH, Khalid AN (2009). Ectomycorrhizae between *Amanita rubescens* and Himalayan Spruce (*Picea smithiana*) from Pakistan. Mycotaxon 107: 73-80.

Oda T, Tanaka C, Tsuda M (1999) Molecular phylogeny of Japanese *Amanita* species based on nucleotide sequences of the internal transcribed spacer region of nuclear ribosomal DNA. Mycoscience 40: 57-64.

Oda T, Tanaka C, Tsuda M (2002). Two new species of *Amanita* from Japan. Mycoscience 43: 351-355

Sánchez-Ramírez S, Tulloss RE, Amalfi M, Moncalvo JM (2015). Palaeotropical origins, boreotropical distribution and increased rates of diversification in a clade of edible ectomycorrhizal mushrooms (*Amanita* section *Caesareae*). Journal of Biogeography 42: 351-363.

Semwal KC, Stephenson SL, Bhatt VK, Bhatt RP (2014). Edible mushrooms of the Northwestern Himalaya, India: a study of indigenous knowledge, distribution, and diversity. Mycosphere 5: 440-461. doi: 10.5943/mycosphere/5/3/7

Singh Y, Kaur M (2016). Two new species of genus *Amanita* from India. World journal of Pharmacy and Pharmaceutical Sciences 5 (5).

Stamatakis A (2006). RAxML-VI-HPC: maximum likelihood-based phylogenetic analyses with thousands of taxa and mixed models. Bioinformatics 22: 2688-2690.

Tibpromma S, Hyde DK, Jeewon R, Maharachchikumbura SSN, Liu JK et al. (2017). Fungal diversity notes 491–602: taxonomic and phylogenetic contributions to fungal taxa. Fungal diversity 83: 1-261. doi: 10.1007/s13225-017-0378-0

Thongbai B, Hyde KD, Lumyong S, Raspé O (2018). High undescribed diversity of *Amanita* section Vaginatae in northern Thailand. Mycosphere 9 (3): 462-494. doi: 10.5943/mycosphere/9/3/3

Thongbai B, Miller SL, Stadler M, Wittstein K et al. (2017). Study of three interesting *Amanita* species from Thailand: Morphology, multiple-gene phylogeny and toxin analysis. Plos One 12: 1-25.

Tulloss RE (2005). *Amanita*—distribution in the Americas with comparison to eastern and southern Asia and notes on spore character variation with latitude and ecology. Mycotaxon 93: 189-231.

Tulloss RE (2009). *Amanita magniverrucata*—revision of an interesting species of *Amanita* section *Lepidella*. Mycotaxon 108: 93-104.

Tulloss RE, Iqbal SH, Khalid AN, Bhatt RP, Bhat VK (2001). Studies in *Amanita* (Amanitaceae) from southern Asia. I. Some species of Pakistan's Northwest Frontier Province. Mycotaxon 77: 455-490.

Tulloss RE, Lindgren JE (1992). *Amanita smithiana*—taxonomy, distribution, and poisonings. Mycotaxon 45: 373-387.

Tulloss RE, Rodríguez Caycedo C (2011). *Amanita* workshop, 6th ed. (amanitabear.com and amanitaceae.org, Roosevelt, New Jersey). 36.

Ullah S, Vizzini A, Fiaz M, Rehman HU, Sher H et al. (2019a). *Strobilomyces longistipitatus* (Boletaceae) newly recorded from Hindukush and Himalayan moist temperate forests of Pakistan. Nova Hedwigia 108: 243-254.

Ullah S, Abbasi M, Khalid AN, Ishaq A, Fiaz M et al. (2019b). *Allodus prostii* comb. nov., causal agent of tulip rust. Nova Hedwigia 108 (3-4). doi: 10.1127/nova_hedwigia/2019/0534

Ullah S (2018). Studies on Basidiomycetes of District Shangla. PhD, Hazara University, Mansehra, Pakistan.

Vizzini A, Zotti M, Traverso M, Ercole E, Moreau P-A et al. (2017). Variability, host range, delimitation and neotypification of *Amanita simulans* (*Amanita* section Vaginatae): collections associated with Helianthemum grasslands, and epitypification of *A. lividopallescens*. Phytotaxa 280 (1): 1-22.

Vilgalys R, Hester M (1990). Rapid genetic identification and mapping of enzymatically amplified ribosomal DNA from several Cryptococcus species. Journal of Bacteriology 172: 4238-4246.

White TJ, Bruns TD, Taylor LJ (1990). Amplification direct sequencing of fungal ribosomal RNA genes for Phylogenetics. In: Innis MA, Gelf DH, Sninsky JJ, White TJ (editors). PCR protocols: A guide to methods applications. New York, USA: Academic Press, 315-322.

Wolfe BE, Tulloss RE, Pringle A (2012). The irreversible loss of a decomposition pathway marks the single origin of an ectomycorrhizal symbiosis. PLoS ONE 7: e39597. doi: 10.1371/journal.pone.0039597

Yang ZL (1997). Die *Amanita*-Arten von Südwestchina. Bibliotheca Mycologica 170: 1-240

Yang ZL (2001). *Amanita pallidocarnea*, a species of *Amanita* section *Vaginatae* with pink lamellae from southeast Asia. Mycotaxon 80: 281-284.

Yang ZL (2002). Revision of *Amanita* collections from Jilin Province, northeastern China. Mycotaxon 80: 67-76.

Yang ZL (2004). Two new species of *Amanita* (Basidiomycota) from China. In: Agerer R, Piepenbring M, Blanz P (editors). Frontiers in Basidiomycote Mycology. Eching, Germany: IGW-Verlag, 315-324.

Yang ZL (2005). Amanitaceae. Fl. Fung. Sin. 27: [1-6], i-xviii, 1-258. [in Chinese.]

Yang ZL (2015). Atlas of the Chinese species of Amanitaceae. Beijing, China: Science Press, 213.

Yang ZL, Cai Q, Cui YY (2018). Phylogeny, diversity and morphological evolution of Amanitaceae. Biosystematics and Ecology Series 34: 359-380

Zhang P, Tang LP, Cai Q, Xu JP (2015). A review on the diversity, phylogeography and population genetics of *Amanita* mushrooms. Mycology 6: 1-5.

Zhang P, Chen ZH, Xiao B, Tolgor B, Bao HY et al. (2010). Lethal amanitas of East Asia characterized by morphological and molecular data. Fungal Diversity 42: 119-133.